Design of Plantar Force Sensor for Ankle Rehabilitation Monitor

By

Evan Downie

Electrical and Biomedical Engineering Design Project (4BI6)

Department of Electrical and Computer Engineering
McMaster University
Hamilton, Ontario, Canada

Design of Plantar Force Sensor for Ankle Rehabilitation Monitor

By

Evan Downie

Department of Electrical and Computer Engineering
Faculty Advisor: Prof. Patriciu

Electrical and Biomedical Engineering Project Report
submitted in partial fulfillment of the degree of
Bachelor of Engineering

McMaster University
Hamilton, Ontario, Canada
April 24, 2010

ABSTRACT

Ankle injuries are one of the most common types of athletic injuries and can have lasting adverse affects on daily life as well as athletic performance without proper rehabilitation and in severe cases can result in chronic ankle instability. Physiotherapy while effective, still employs many techniques that are largely qualitative for lack of an easily accessible system that can offer a quantitative approach. The design of an ankle rehabilitation monitor seeks to provide a fast, effective, affordable and repeatable method of acquiring qualitative data of importance when diagnosing and treating injuries related to the ankle. Plantar forces acting on the sole of the foot represent a set of data that can be important to a practitioner but are difficult to acquire without specialized equipment, and as such are part of the focus in the design of an ankle rehabilitation monitor. The device strives to provide a physiotherapist with plantar force measurements using a set of force sensing resistors affixed to a shoe insert that can be retained and compared in order to track the rehabilitation of ankle related injury. A proof of concept utilizing three such resistors is implemented and demonstrates that this approach is a reasonable design. The theory behind the device and its hardware and software design, experimental results, and efficacy are presented within.

Key words: plantar force, in-shoe plantar force measurement, ankle injury, rehabilitation, force sensing resistor, FSR, gait analysis.

Acknowledgements

Thank you to Dr. Patriciu first and foremost for supervising the project and guiding the design process. His knowledge of engineering design was invaluable over the course of this project and very important to someone who has no previous experience with a formal engineering design project.

Thank you to Rakefet Hootnick, a physiotherapist with the McMaster athletics and recreation department, for providing insight into the biomechanical and physiotherapy-related aspects of the project and suggestions regarding the design direction. Your assistance in the research of physiotherapy and biomechanics related to the project was also a great help.

Thank you to Ryan Keyfitz, who worked on the ankle range of motion portion of the project for his support throughout the course of the design project, and for his contribution of the idea for this project.

Finally, thank you to everyone else who assisted along the way, including, but not limited to, Mike Willand and the course TA, Saba Mohtashami, for assisting with the some of the work done in Labview, and to Dr. Doyle for coordinating the design course and poster fair.

Contents

List of Tables

List of Figures

Nomenclature

ADC	Analog to Digital Converter
Distal	In anatomy, meaning part of a structure away from the trunk of the body.
FSR	Force Sensing/Sensitive Resistor
Hallux	Anatomical term for the big toe.
Hysteresis	The lagging of an effect behind its cause.
Inferior	In anatomy, meaning away from the head, lower part of a structure, or below.
LabVIEW	Programming environment used to produce signal analyzing and other specialized systems virtually.
Lateral	In anatomy, perpendicular to transverse and coronal planes but not along the medial plane, away from the medial plane.
Medial	In anatomy, along the medial axis, looking outwards.
NI	National Instruments
PFS	Plantar Force Sensor
Proximal	In anatomy, meaning part of a structure nearer to the trunk of the body.
Superior	In anatomy, meaning towards the head, upper part of a structure, or above.
Transverse	In anatomy, meaning a plane separating the body or structure into superior and inferior halves.
VI	Virtual Instrument, a program created in the LabVIEW environment.

CHAPTER 1

INTRODUCTION

1.1 Background

Ankle injuries are one of the most common types of athletic injuries and can have adverse affects on daily life as well as athletic performance. Proper rehabilitation of an ankle injury is important in order to prevent long term persistence of these affects. Balance, proprioception and range of motion can be negatively affected due to ankle injuries and in severe cases chronic ankle instability can occur. It is important to know the physiology and biomechanics involving the ankle in order to assess and treat an injury. The range of motion, ankle torque and plantar forces are some of the pieces of information that contribute to this understanding.

The acquisition of plantar force has been an important part of gait and stance analysis in the past, and as such various experiments to record this data have been performed. Gait and stance analysis play a large role in the rehabilitation of ankle injury and management of symptoms in diseases such as cerebral palsy or the effects of aging [1]. It follows that gait analysis techniques are numerous and several devices do exist to extract this data using a variety of methods. Many methods are bound to a laboratory and require a user to walk in a specified pattern or along a specific contour while other methods have become less restrictive and cumbersome [2]. However none of these methods take into account the position of the lower leg relative to the foot and the plantar force alone does not accurately portray joint position, though experiments that consider shear forces are attempting to fulfill this need [3]. By combining the plantar force analysis with ankle range of motion analysis during gait and other activities perhaps more insight into the onset and pathology of problems with the ankle joint and gait can be provided.

Devices such as these are often used in a clinical environment by physiotherapists and other medical or research staff. Specifically in the practice of physiotherapy, gait and range of motion information are very important diagnostic tools used to determine

appropriate treatments and assessments. However, some of the practices in this field have qualitative aspects that rely heavily on the aptitude of the practitioner and as such the interpretations and results of many tests can differ between individual physiotherapists [4]. In the case of musculoskeletal injury, assessments often involve viewing movement of the affected region, examining the muscles by hand to feel for abnormalities and determining the level of pain associated with the injury [5]. This approach can be sufficient for many injuries, but quantitative assessments could help improve the consistency of diagnoses among physiotherapists.

Existing in-shoe plantar force sensors use a variety of force transducers, sensors and modalities. Most modern systems are attached to a shoe and either use a force transducer matrix or affix sensors to specific anatomical landmarks, though attaching sensors to a sole is also used in some commercial systems such as the F-Scan system. Many of these implementations are used to track the effect of footwear on the walking cycle rather than to analyze normal gait, and no commercially available system incorporates ankle torque or range of motion information in the same device. Additionally, the systems that are available are quite expensive due to the cost and complexity of transducer arrays and as such are not widely used.

1.2 Objective

The objective of this device is to provide physiotherapists with a means to acquire information from the usual tests in a quantitative way to accompany their qualitative analysis and provide a constant measurement to use between rehabilitation assessments that is easy to use and inexpensive. This report focuses on the design of the plantar force sensing component of a system that will measure those forces as well as the range of motion of the ankle. The device needs to operate without affecting any of the variables of the qualitative analysis while measuring the plantar forces at important anatomical sites on the foot. The data acquired should be accompanied by a robust computer interface and be able to be manipulated in a variety of ways such as writing to a file, storage, reading from stored files and comparison between data in real time and in archives. Section 1.2.1 details the concise specifications of the device.

1.2.1 Design Specifications

The device and software should:

- Be able to measure forces caused by applied weights up to 100 kg.
- Be precise in measurements to less than or equal to 1 kg.
- Provide repeatable results to within an error of 5%.
- Have a total cost of less than $100 CAD.
- Not affect natural gait, comfort, or range of motion of the ankle during use.
- Fit comfortably into normal footwear.
- Be able to record, store and compare data acquired from the PFS.
- Sample data at a rate of 1000Hz.
- Not require any knowledge of software or programming to use.

1.3 General Methodology and Scope

The goal of this project is to produce a working proof of concept of a PFS for use in an ankle rehabilitation monitor. This includes producing the sensor device that can be inserted into footwear along with the range of motion monitor, the circuit and power supply to produce a useful signal from the device and the programming of the graphical user interface. The design process of this project can be broken up into three sections.

1.3.1 The Force Sensor

The first part of the design was to choose a device that can measure forces as defined in the specifications. Research on force sensing devices yielded several high precision, high maximum input range devices but these strain gauge devices violate the specification of not affecting movement due to their size, while force transducer matrices or films are far too expensive. Piezoresistive force sensing resistors (FSR) however are very thin, flexible sensors that are also moderately priced and can be adjusted for different force ranges and thus were the most suited for the force sensor in the ankle rehabilitation monitor. Once a circuit was designed to use the sensors, each FSR would need to be calibrated, and the relationship between force and resistance determined on an individual basis. Once

calibration was complete, the sensors could be affixed to positions on a simple store bought insole and wired to their respective circuits.

1.3.2 The Circuitry

Because each FSR is likely to have slightly different behaviour, each sensor requires its own drive circuit. The drive circuit is a standard inverting amplifier circuit or current to voltage converter, with the FSR wired to the input and the gain resistor wired between the negative terminal of the OP-AMP and the output. The gain resistor determines the sensitivity of the sensor and would need to be tuned based on the calibration data. The output voltage of the circuit should be suitable for conversion by most microchip's ADC which is between 0 V and 5 V. Once a circuit had been designed it would be soldered to a circuit board alongside the ankle range of motion monitor circuit and voltage regulation circuitry.

1.3.3 The Data Acquisition and Graphical User Interface

In this design the voltage read from the circuit is converted to digital data by the National Instruments (NI) ADC where it is acquired by the associated software called LabVIEW in a custom designed virtual instrument (VI). Once converted to a digital signal, the voltage data must be equated to a force input to the system and displayed on screen for the user. The data manipulation options outlined in section 1.2.1 must be met, and embodied in an easy to use executable file. A VI designed for the PFS as a standalone device and as a combined ankle rehabilitation device is implemented with contributions from the ROM monitor system.

CHAPTER 2

LITERATURE REVIEW

2.1 Plantar Forces

In order to design a product to measure plantar forces it is important to understand what kinds of forces are expected and the motions of the body that produce them. The term plantar forces refers to the forces occurring on the undersurface of the foot which includes shear forces but in the context of this report refers only to vertical forces. These forces are not constant and can vary greatly both in magnitude and distribution depending upon the actions of the subject and can total between zero and five times the weight of the human body [5]. Because it is an enormous undertaking to classify every possible motion and its resulting distribution of plantar forces the most common method of study is during the few defined sets of movements such as standing or during gait. Even these defined sets of motions do not produce consistent plantar force distributions between subjects, as the posture and structure of the foot also affect these values. Common types of foot structure are neutrally aligned, where initial contact in running or gait begins with a heel strike followed by onset of forces from heel to toe, and pes planus or flatfeet, where the arch of the foot has not developed and the entire sole of the foot makes contact with the ground, both conditions have slightly differing force distributions [6]. Because of the variation between individuals it is most effective to compare plantar forces between asymptomatic and symptomatic feet of the same subject when possible.

Once a set of movements is defined measurements of plantar force between trials become more meaningful. An illustrated demonstration of the common gait cycle can be found in Appendix A.1 and labels the stages of common gait. These motions are often used when comparing subjects to determine the effects of abnormal conditions. During the aforementioned gait cycle it is expected that the heel strikes the ground first during the initial contact phase, followed by a rolling motion from the hindfoot along the midfoot and ending at the forefoot during the loading response. When the opposite leg is raised, the foot is said to be in the midstance after which the opposite leg enters the initial

contact and the foot enters terminal stance. These stages of gait are referred to as the stance phase and are the common duration of a plantar force measurement. A study performed by Lidoux and Hillstrom appearing in Gait and Posture found the average plantar force distribution during the stance phase in Figure 2.1 [6]. As can be seen in the

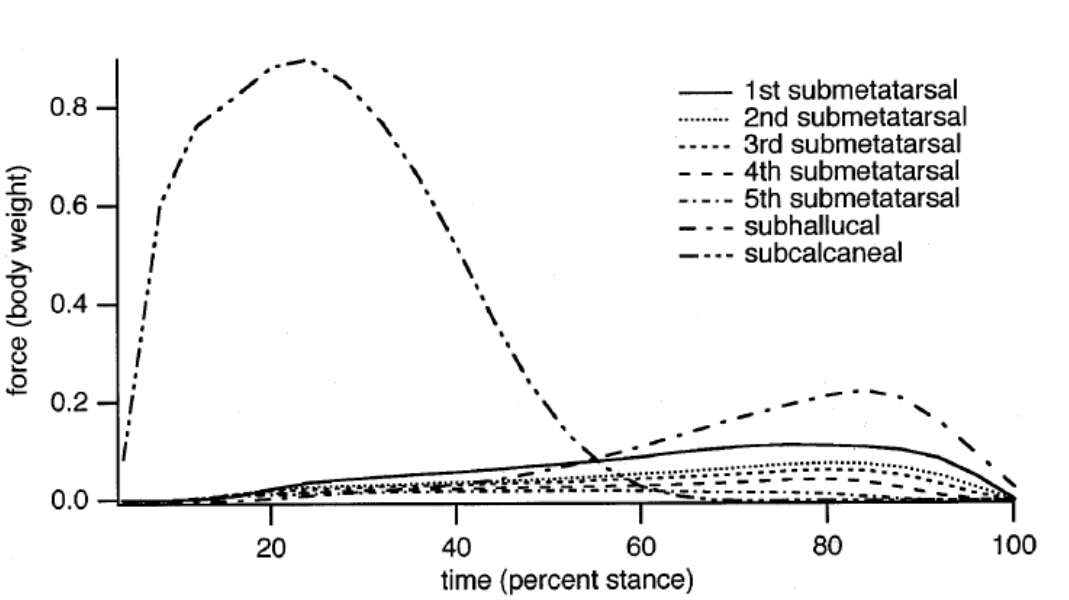

Figure 2.1 – Average force versus percent stance curves for 10 trials of a typical subject (left foot, neutrally aligned). [6]

figure, the forces in the heel region are much higher than the rest of the foot for the first sixty percent of the stance phase which follows logically from the heel being the initial contact point. The subhallucal forces refer to the forces under the big toe and are the second largest in magnitude occurring in the final forty percent of the stance phase which follows logically from the big toe being the point of take off as illustrated in Appendix A1 in the preswing phase. The aforementioned study used pressure plates to acquire these values and the goal was to compare neutrally aligned feet and pes planus feet, the results of which can be seen in Table 2.1 [6]. The table shows the only significant difference between flat footed persons and normal neutrally aligned persons is the force distribution at the hallus. This could still be significant in physiotherapy when designing specialized orthotics.

The real purpose of plantar force measurements is to compare between symptomatic and asymptomatic individuals. A study comparing the plantar forces of

Table 2.1 – Peak force in body weight between neutrally aligned and pes planus feet. Significant differences denoted by an asterisk. [6]

Location	Neutrally aligned	Pes planus	*P*-value
(a) Peak force (body weight)			
1st submet	0.318	0.346	0.3095
2nd submet	0.329	0.331	0.9070
3rd submet	0.239	0.233	0.6356
4th submet	0.186	0.174	0.4075
5th submet	0.117	0.106	0.3978
Subhall	0.195	0.253	0.0064*
Subcalc	0.973	0.924	0.0882

persons with chronic ankle instability and asymptomatic persons was performed by Nyska et al. for the Journal of Sports Medicine and had more significant findings [7]. Table 2.2 shows their results and indicates that those with chronic ankle instability have significant increases in duration of plantar pressures at different locations during gait with significantly altered distributions of those forces. Another conclusion drawn by the study was that those with unilateral ankle instability had their asymptomatic foot affected as well in most cases, which further stresses the need to be able to quantify these differences for more relevant comparisons between subjects.

Table 2.2 – Percentage of total stance time in patients with chronic instability of the ankle and controls (top). Forces in body weight in patients with chronic instability of the ankle and controls (bottom). [7]

	Controls	Injured	p Value
Number of patients	12	12	–
Number of feet examined	24	17	–
Central forefoot	17.88 (1.68)	18.83 (1.22)	<0.01
Lateral forefoot	15.47 (1.98)	16.87 (2.04)	<0.05
Toes	16.56 (0.42)	17.03 (0.38)	<0.05
Number of patients	12	12	–
Number of feet examined	24	17	–
Heel	0.744 (0.066)	0.700 (0.094)	NS
Midfoot	0.158 (0.07)	0.207 (0.089)	<0.05
Lateral forefoot	0.224 (0.065)	0.0269 (0.068)	<0.05
Toes	0.292 (0.109)	0.214 (0.08)	<0.01

Values are mean (SD).

2.2 Measuring Plantar Forces

There are a variety of ways to measure forces but not all methods are suitable for physiological measurements and fewer are suitable for measuring plantar forces. Load cells and strain gauges are typically able to offer fine precision and can be designed to sustain large weight loads which but have larger space requirements, and in the case of conventional strain gauges very specific orientation requirements. This makes them suitable for measurements that can accommodate these requirements, but plantar forces are very susceptible to abnormal surfaces since the sole of the foot is not extremely elastic [6]. As such more subtle devices need to be used in the design of an in shoe PFS which leaves force sensitive resistors and a less direct method using pressure transducers.

2.2.1 Pressure Transducers

A strain gauge is a type of pressure transducer and part of a classification of sensors that convert pressures to an electric signal. A common form of pressure sensor is one that measures the change in gaseous pressure inside of a device which can be attached to a sealed envelope and used to measure forces acting on the outside of the envelope. Devices such as the Freescale© MPX5050[1] operate by using a small transducer inside of a device with higher pressure on one side and lower pressure on the other with the input connected to a port on the device. The pressure is determined by the transducer due to the pressure differential causing a deformation of the transducer and producing a current in the same manner that deforming a strain gauge does. This technology was considered as an alternative to FSRs but ends up making the design needlessly complex. A sole would need to be designed with specialized pockets instead of sensors over each area of interest with a leading hose to the input to the transducer, one for each pocket. While these types of sensors can be very accurate over their range they can also be very temperature sensitive. The MPX5050 includes temperature compensation within the device but it still contributes to the error percentage of ±2.5% of the full scale voltage of 5 V. The cost is moderate at $11 CAD for individual orders, but that does not factor in the cost of fabricating the sole.

[1] http://www.freescale.com/files/sensors/doc/data_sheet/MPX5050.pdf

2.2.2 Force Sensitive Resistors

Force sensitive resistors are well suited to this application due to their thickness and the ability to detect a large range of forces based on the design of the circuit. FSRs are a polymer thick film device and use a relatively simple technology to convert forces into changes in resistance within the sensor which is demonstrated in Figure 2.2 [8]. The layer

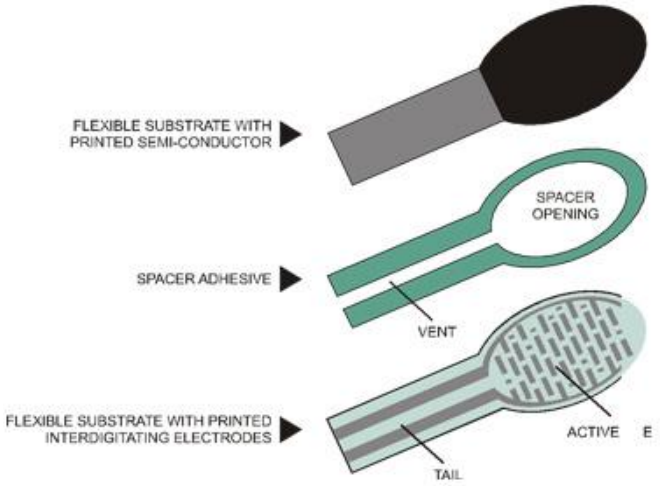

Figure 2.2 – Layers of a polymer thick film FSR, showing the vent, tail and electrode layouts. Interlink Electronics FSR shown. [8]

of flexible substrate with a printed semi-conductor is separated from the corresponding layer containing electrodes by a spacer layer filled with air. When force is applied, the pressure is regulated by the vent, and the semiconductor begins to connect with the electrodes allowing current to flow, with a resistance determined by the conductive polymer semiconductors in proportion to the pressure applied to them [9]. A typical resistance versus force curve is given in Figure 2.3, though the range varies between sensors [10]. The sensors have very low temperature sensitivity in the range of 0 to 65 ^{o}C which is ideal for physiological settings and the sensitivity can be controlled by the circuit set up, which is described further in Chapter 4. The devices may operate as a simple switch in voltage division circuits or as a quantitative sensor in current to voltage converter circuits.

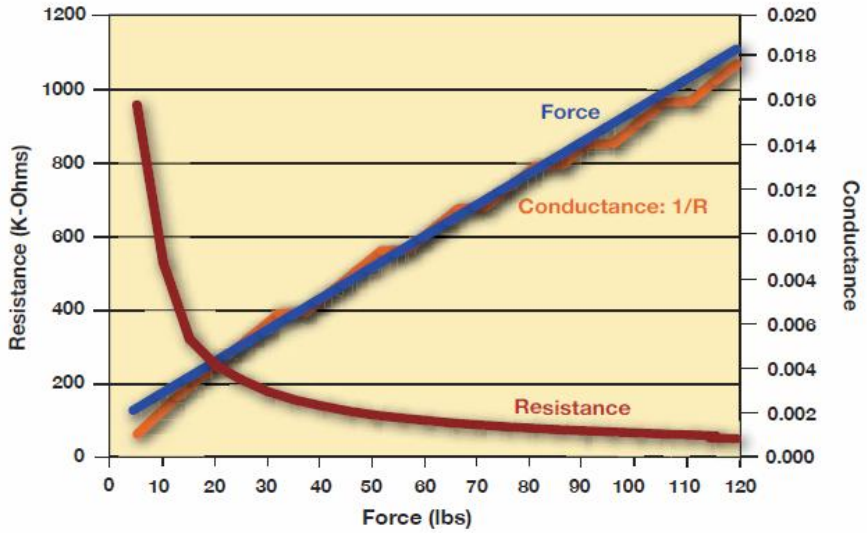

Figure 2.3 – Resistance and conductance versus force for the 100lbs Flexiforce FSR produced by Tekscan. [10]

There are two common commercial suppliers of FSRs that produce slightly different variants of the sensor, Interlink Electronics and Tekscan. Tekscan produces a sensor called the Flexiforce sensor and has a multitude of force ranges available in customizable arrangements, while Interlink Electronics FSRs are available in a variety of shapes and sizes with a typical resistance curve similar to that of Figure 2.3. However the Interlink Electronics variety indicates resistance saturation at only 10 kg of applied weight. Both sensors can be manipulated to provide more desirable ranges and sensitivities based on the supply voltage and reference resistance used in the suggested current to voltage converter circuit which can be seen in Figure 2.4 [8]. Both sensors are extremely thin at 0.46mm for the Interlink Electronics FSR and 0.208mm for the Tekscan Flexiforce sensor, either of which could measure plantar forces without any effect on the natural distribution or motion.

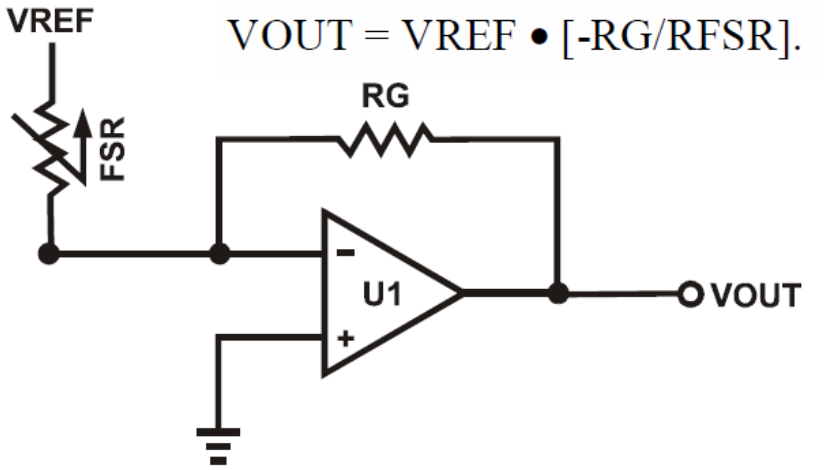

Figure 2.4 – Current to voltage converter current. Reference resistor labeled RG, FSR depicted as a resistor, and U1 represents any generic OP-AMP. [8]

The shortcomings typical of FSRs are the level of hysteresis, defined as lag between applied forces and their effect, drift in the sensors nominal resistance and response to shear forces. These commercially available FSRs have been refined to reduce these values significantly, however a study performed by Hollinger and Wanderley at the input devices and music interaction laboratory at McGill University found the characteristics of the Interlink Electronics FSR to be superior [11]. The average drift over 240s with varying loads of the Interlink Electronics FSR was 7.71% of maximum output, while the Tekscan FSR had an average 10.88% drift, though for repeated 1 kg loads the drift was lower in the Tekscan FSR. Additionally, the hysteresis of the Flexiforce was found to be consistently higher and actually increased after repeated testing [11]. These factors alone would make the Interlink Electronics FSR the clear choice for this design project, but it also costs less per unit than the Tekscan Flexiforce, and as such were used in the PFS design.

CHAPTER 3

PROBLEM STATEMENT AND METHODOLOGY OF SOLUTION

Physiotherapy includes many tests and practices that are qualitative and depend largely on the skill of the practitioner. These tests are used to acquire valuable information regarding the pathology of a range of possible injuries and afflictions such as joint injury, fracture recovery, and Parkinson's disease [2]. The ankle in particular is an extremely common site of injury, and can have lasting effects if not treated properly [12]. Physiotherapy involving the ankle is often concerned with the range of motion and forces acting on the joints in order to provide the information required to produce orthotics, braces and other injury and anatomy specific rehabilitation devices. In order to improve consistency among test outcomes quantitative information regarding the biomechanics of the ankle could be produced alongside the qualitative results to provide more robust diagnoses.

Gait is a subject of much analysis when it comes to treating a variety of ankle injuries but is not limited to those types of injuries alone; Parkinson's disease and diabetes have many adverse affects on gait [13][14]. Proper analysis of gait requires more than subjective analysis and often includes evaluations of lower limb mobility, foot deformities, trunk and pelvic posture, knee and heel position, plantar foot arch and plantar force measurements (often in three dimensions) [14]. Specialized equipment is required for measuring most of these values and mobility and plantar force are no exception. This project focuses on addressing the problem of measuring plantar forces as part of a specialized system to analyze both ankle mobility and plantar force.

3.1 General Problem

While there does currently exist specialized equipment to measure plantar forces for use in gait analysis they do possess certain shortcomings mentioned previously in section 1.1 that limit their widespread use. The result is that there is currently no plantar force sensing device that can provide accurate and useful information about the forces acting

on the foot that is also cost effective enough to be available to every physiotherapy practice regardless of size and resources. There currently exists no commercially available device that meets the aforementioned criteria that also incorporates useful information about the mobility of the ankle.

3.2 Methodology of Solution

3.2.1 Placement of Force Sensors

Without using a transducer matrix or film, a layer cut to the exact shape of the foot that gives force data at high resolution throughout, sensor placement becomes very important in order to provide useful information without receiving information from the entire area under the foot. While specific locations of abnormal or increased plantar forces are important, physiotherapy is concerned with forces affecting the three major divisions of the foot, the hindfoot, midfoot and forefoot [5]. Figures 3.1 and 3.2 show medial and superior transverse views of the foot and ankle taken via x-ray imaging and identifies the major bone structures within them. The figures have been modified slightly to indicate the approximate separations between the regions of the foot. The joints formed between these bones are what separate the foot into the three regions, as defined by Table 3.1. These regions are generally accepted as defined here, though the proximal heads of the metatarsal bones can sometimes be considered to be within the midfoot as well.

Figure 3.1 – Medial view of the human foot, taken by x-ray photography. Bone structures are indicated in red. Approximate separations regions between regions of the foot are shown in blue. [15]

Figure 3.2 – Superior transverse view of the human foot, taken by x-ray photography. Bone structures are indicated in red. Approximate separations between regions of the foot are shown in blue. [15]

Table 3.1 – Structures comprising the hindfoot, midfoot and forefoot [5][16].

Region of Foot	Structures Defining the Region
Hindfoot	The most proximal part of the foot, containing the calcaneus, Achilles tendon and the ankle, talocalcaneonavicular, calcaneocuboid and cuneonavicular joints.
Midfoot	The midfoot lies between the hindfoot and forefoot, containing the subtalar joint, talocalcaneonavicular joint, cuneonavicular, calcaneocuboid, cuboideonavicular, cuneocuboid, intercuneiform and tarsometatarsal joints.
Forefoot	The most distal part of the foot, containing the toes and the interphalangeal and metatarsophalangeal joints.

In order to provide useful information about the plantar forces acting on the foot, sensors would need to be placed in each of these three regions. Forces are distributed across almost the entire area of the foot, but the largest forces occur in the areas under the calcaneus, the hallux (big toe), along the lateral-most metatarsal and along the distal metatarsal heads and thus these positions are prioritized when working with a small number of sensors [6]. Using only three FSRs in the proof of concept, the highest priority locations of interest are under the calcaneus to represent the hindfoot, under the proximal head of the 5^{th} (lateral most) metatarsal to represent the midfoot, and under the distal head of the 1^{st} (medial most) metatarsal near the sesamoid bones to represent the forefoot [6]. These locations correspond to those seen in Figure 2.1 on page 6, though do not include the hallux. The reason for this is that the hallux is in the distal portion of the forefoot and the total force over the metatarsal heads is comparable, it is important for symptomatic cases to get an idea of those forces. As more sensors are added, they would be affixed beneath hallux firstly, the distal heads of the 2^{nd} through 5^{th} metatarsals secondly and lastly along the lateral side of the midfoot as these are the remaining areas of notable weight bearing, in order of magnitude [6]. Sensors affixed to these locations would likely give a practitioner enough quantitative data to proceed with a diagnosis or treatment plan.

3.2.2 Choice and Cost of Force Sensors and Insole

In order to accurately measure plantar forces the device used to do so cannot impede or affect the natural distribution of those forces. If there is any non-uniformity in the device when beneath the foot, it could greatly affect the distribution of forces in the same way that walking on an abnormal surface would [6]. Thus the sensors themselves as well as the insole containing them must be uniformly distributed and very thin.

Luckily, the cost of a commercially available insole is proportional to the effectiveness of the orthotic and thus the non-uniformity, in short, the more uniform and thin the insole, the less costly it is. The insole chosen for this design project was the Dr

Scholl's Air-Pillo[2] cushioning insoles, a uniform insole that is 3.1mm in thickness at a cost of $4 CAD. This insole satisfies all the criteria required to allow the sensors to perform without affecting the measurements significantly.

The choice of force sensor was not as simple as there are many more factors to consider. The sensor used in the design of the PFS was the Interlink Electronics[3] series of force sensing resistors, namely the 1.5" (3.81cm) square FSR and the 0.5" (1.27cm) diameter circular FSR. These sensors are available for $9.48 CAD and $6.95 CAD respectively, with thicknesses of 0.46mm throughout. When affixed to the insole the difference in thickness would be negligible and as such these sensors are well suited to the design in this aspect. A more in depth analysis of the choice of sensor for this project is found in chapter 2, literature review.

These products satisfy the requirements of the theory related to the operation of the PFS and will allow for proper measurements of plantar force with regard to their placement and affect on results.

[2] http://www.drscholls.com/drscholls/productSearch.do?method=doProductDetailsLookup&searchArg=58
[3] http://www.interlinkelectronics.com/force_sensors/products/forcesensingresistors/index.html

CHAPTER 4

DESIGN PROCEDURE

4.1 Circuitry Stage

The circuitry to be used for each sensor begins with the circuit described in Figure 2.4, a current to voltage converter also known as an inverting amplifier. When using these sensors the choice of the reference resistor is important because it sets the sensitivity of the sensor response. This is because as the sensor resistance is driven lower the change in resistance per unit of force applied gets smaller, as indicated by Figure 2.3, and these changes in resistance are reflected in the output voltage proportional to the percentage change compared to the reference resistance. Since the PFS needs to measure heavy loads that may be outside the listed range of the sensor, the reference resistance must be very low.

The drive voltage is another important choice in designing the circuit, since the sensors have limits on the amount of current that can pass through them without damaging the device. The Interlink Electronics FSR guide states that current through the device should be limited to 1 mA/cm^2, which limits the current in the sensors used to 14.52 mA for the square sensor and 3.98 mA for the circular sensors. With this knowledge it was possible to determine the drive voltage and reference resistance to be used.

An inverting amplifier circuit was set up using a 1 kΩ resistor as reference and a 0.5 V DC drive voltage. Each sensor was arranged in the circuit as previously described and then actuated with as much force as possible in order to drive the resistance to saturation and the output voltage was observed. Force was applied by piling weights onto a small disc covering the surface area of the sensor until the output voltage began to saturate, similar to the procedure described in section 4.2 used to calibrate the sensors. Using the output voltage and the equation described in Figure 2.4, the approximate saturation resistance could be determined and the results can be found in table 4.1.

Table 4.1 – Tabulated results from determining saturation resistance. Maximum drive voltage calculated using proposed maximum currents of 14.52mA and 3.98mA.

Sensor	**Output Saturation Voltage (mV)**	**Approximate Saturation Resistance (Ω)**	**Calculated Maximum Drive Voltage (mV)**
1.5” (3.81 cm) square	8801.2	56.81	824.88
0.5” (1.27 cm) dia. circle #1	1380	362.31	1441.99
0.5” (1.27 cm) dia. circle #2	1400	357.14	1421.41
0.5” (1.27 cm) dia. circle #3 (extra)	1412.7	353.92	1408.6

The circuit was to be powered by a pair of standard 9 V batteries, used to power the OP-AMPs (LM 741 and OPA2336) supplied by McMaster University and the rest of the circuit elements as well as the drive voltage. As mentioned, there are proposed current limits on the sensors which combined with the saturation resistance gives a maximum drive voltage given in Table 4.1 above. Unfortunately the lowest output voltage regulator available for the design was the National Semiconductors LM317T variable voltage regulator which had a minimum output voltage of 1.25 V, which satisfies the requirements for the circular FSRs but not the square. After further testing it was determined that the increased current is within a safety factor for the maximum proposed current of 1.51 and seemed to have no effect on the sensor operation. This voltage regulator also only operates with positive voltage bias, which meant the output of the inverting amplifier would have to be negative, which is not ideal for many ADC devices.

Since a range of 0 to 5 V is acceptable in almost all ADCs on microchips, this meant that the OP-AMPs were to be powered using ±5 V and that the maximum gain of the circuit given a 1.25 V drive voltage was 4. So the choice of reference resistor was made to be approximately double the saturation resistance of the corresponding sensor, and a second inverting amplifier with a gain of 2 would be added. The output of these stages is fed into the NI ADC for use in the program component of the design.

Two Fairchild Semiconductors KA78M05 positive 5 V voltage regulators were used to limit the voltage to the OP-AMPs to ±5 V by taking advantage of the virtual ground on the circuit board and reversing the inputs on one regulator with one of the 9 V supplies. All of these elements were soldered onto a circuit board alongside the ankle range of motion circuitry to allow for mobility in future modifications such as using a microchip ADC instead of the NI ADC. The final circuit board can be seen in Figure 4.1.

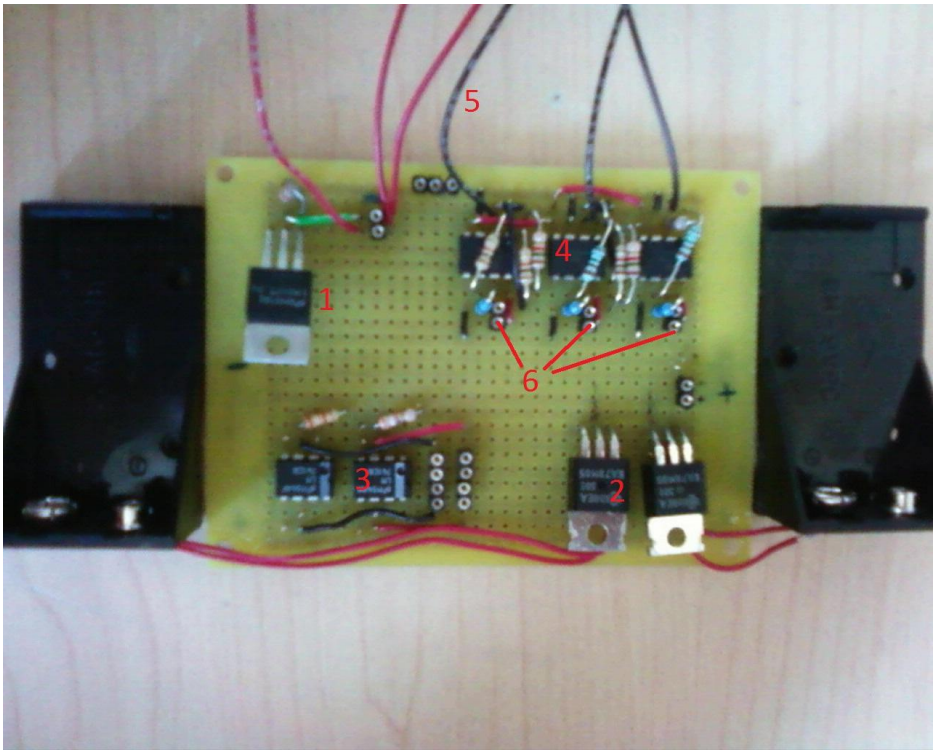

Figure 4.1 – Circuit board containing circuitry and power for PFS and range of motion sensor. (1) The LM317T variable voltage regulator, set to 1.25V. (2) The KA78M05 5V voltage regulators. (3) Circuitry for ankle range of motion sensor. (4) Circuitry for PFS. From right to left, dual OP-AMP chips for the square hindfoot sensor, circular midfoot sensor and circular forefoot sensor. Reference resistances for first inverter were 100Ω and 600Ω respectively. Second inverter used 1k and 2k resistors to give gain of 2. (5) Leads to connectors to attach the PFS device. (6) Pin connectors to wire into the NI ADC.

4.2 Calibrating the Sensors

Once the circuit had been constructed on a breadboard the next step was to determine the force to resistance characteristics of the sensors. The sensor properties do vary slightly in this sense so for most accurate results each sensor needed to be calibrated individually. During the calibration each sensor was attached to its corresponding circuit and actuated by a series of increasing weights while it was attached to the sole at locations described in section 3.2.1 in order to get a more realistic representation of the output of each sensor while it is in use inside of a shoe. The weights were placed sequentially on top of a cylindrical 1 kg weight used to distribute the force over a 5cm diameter centered on the sensor as seen in Figure 4.2. The voltage output was used to calculate the resistance vs.

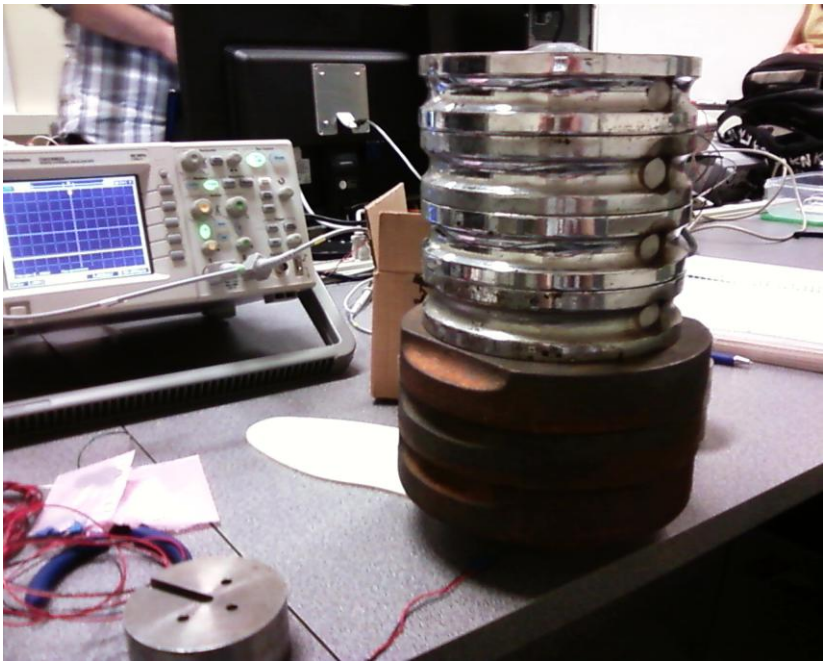

Figure 4.2 – Weights actuating sensor beneath the sole of the PFS. Picture shows 33.68kg in circular weights aligned with the center of the sensor. Output displayed on oscilloscope.

voltage curve, however since the circuit was suitable for the sensors and their range, to simplify calculations within the program a relationship between the output voltage of the circuitry and the applied weight was determined. Using MatLAB software, a 4^{th} degree polynomial curve relating these two values was calculated in order to interpolate the applied weight corresponding to voltage outputs that had not been tested. The equation of

these curves and their residuals, or error at known points, is displayed in figure 5.1 on page 24 showing the results of the experiment for the three sensors used in the initial PFS design. These polynomial equations were then used in the next stage of the design, the LabVIEW virtual instrument.

4.3 LabVIEW Design

With the fitted curve equations and circuit design determined, the final stage of the project was to design a graphical user interface to use with the PFS tool to display meaningful results to a user on their computer. This interface was designed using the LabVIEW environment and reads from the NI ADC to receive the data from the sensors. As per the design specifications, the program allows a user to manipulate the data in a number of ways including saving and comparing previously recorded measurements, scrolling through the time axis to examine signals of interest, and viewing the sensor readings individually to isolate one section of the foot or all together. In addition to these features, the program uses the formulae determined in section 4.2 to display a graph of applied weight in kilograms versus time in seconds from the digital voltage measurements received from the ADC. A LabVIEW VI is split into two parts; the interface is called the front panel and is what the user interacts with, and the program code is arranged in a block diagram that operates behind the front panel to execute the program. The block diagram of the programs designed for this project can be found in Appendix A.3. Two programs were designed to fulfill the specifications, one to act as the interface for the PFS on its own, and one to incorporate the ankle range of motion sensor data designed by Ryan Keyfitz. It is important to note that even though these programs are compiled into a windows executable file, the LabVIEW environment is required on the computer in order for the programs to run.

4.4 Complete Design

With all of the components of the system designed and implemented separately, all that is left is to combine them to produce the operational PFS tool. A block diagram displaying how the sections of the device interact is seen below in Figure 4.3 and shows the inputs and outputs of each stage of the system.

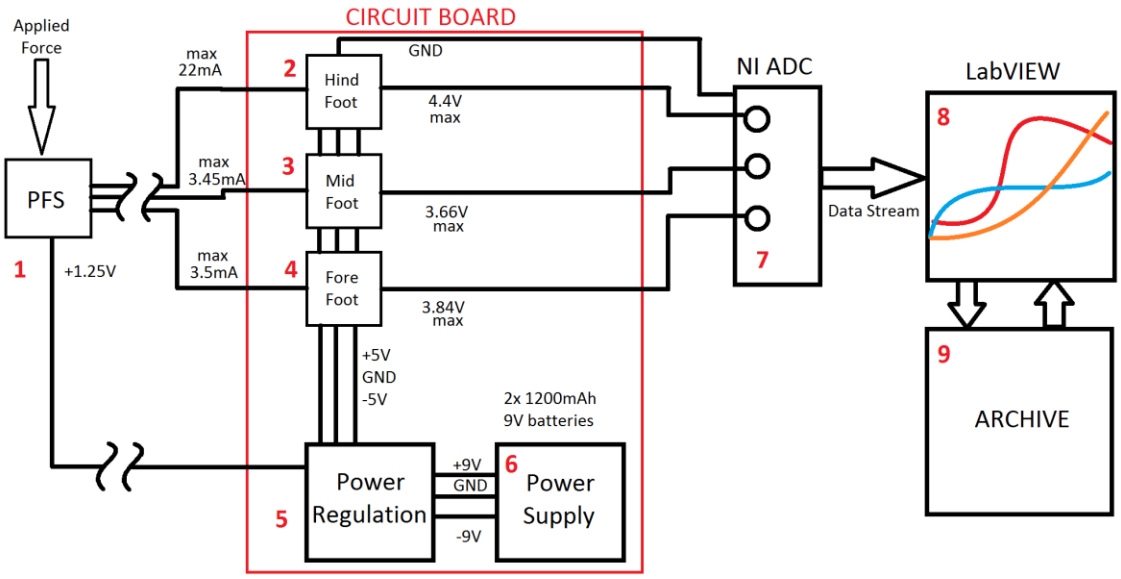

Figure 4.3 –System diagram showing each block of the plantar force sensor system and the inputs and outputs from each of them. (1) PFS block represents the sole containing the force sensors that converts applied force into a current signal. (2) Hindfoot circuitry containing two consecutive inverting amplifiers that facilitate the sensor's quantitative property as opposed to qualitative (switch) and amplify the input current into a suitable voltage range. (3) Midfoot circuitry works much the same as the hindfoot block, as does (4) the forefoot block. (5) Power regulation block regulates the power supply to ±5V and +1.25V. The ±5V supplies are fed into the OP-AMPs in blocks 2 to 4, and the 1.25V voltage is dropped across the sensors in the PFS block. (6) Power supply block contains 2 Energizer 9V lithium batteries with 1200mAh supplies. (7) The NI ADC which converts voltage signals from blocks 2 to 4 into a data stream for use by block 8. (8) The LabVIEW VI is present on a computer attached to block 7 and displays the signals as applied force versus time on screen. (9) Computer memory block that holds archived measurement files from block 8.

CHAPTER 5

RESULTS AND DISCUSSION

5.1 Results

The sensors provide readily repeatable values, but the orientation of the weight on the sensor has a large effect on the resulting resistance of the FSR. During testing, weight was distributed evenly over the surface of the FSR and values were consistent within 5% over the range of expected values. During testing the square FSR reached a steady resistance of ~58 Ω at an applied weight $\geq$ 33 kg while the circular FSRs reached a steady resistance of ~360 Ω similarly, at 38 kg. The results of testing can be seen in Figure 5.1 which shows the fitted curve on top of the actual data in order to display its relative accuracy, though it should be noted that outside the range of experimental values these equations are not accurate for use in extrapolation. These values fall short of the desired 100 kg range but do satisfy the sensitivity requirements as defined in section 1.2.1.

Unfortunately, in regular human movement there are shear forces which slightly alter the behavior of the FSRs, further diminishing the range of forces picked up by the sensors during intended use. During operation of the device the hindfoot sensor reaches a maximum value corresponding to ~25 kg while the mid and forefoot sensors reach a value corresponding to 40 kg faster than anticipated, but only when force is applied precisely over only the sensor area which does not regularly occur during normal gait while using the device. The result of two full gait cycles can be seen in Figure 5.2 displayed on the LabVIEW VI front panel that the user interacts with. While the values for the heel should typically be as much as 95% of the body weight while the plot only reaches 25 kg at a maximum, the timing and body weight proportion of the mid and forefoot appear to agree with Figure 2.1 on page 6 for the 75 kg subject that was used.

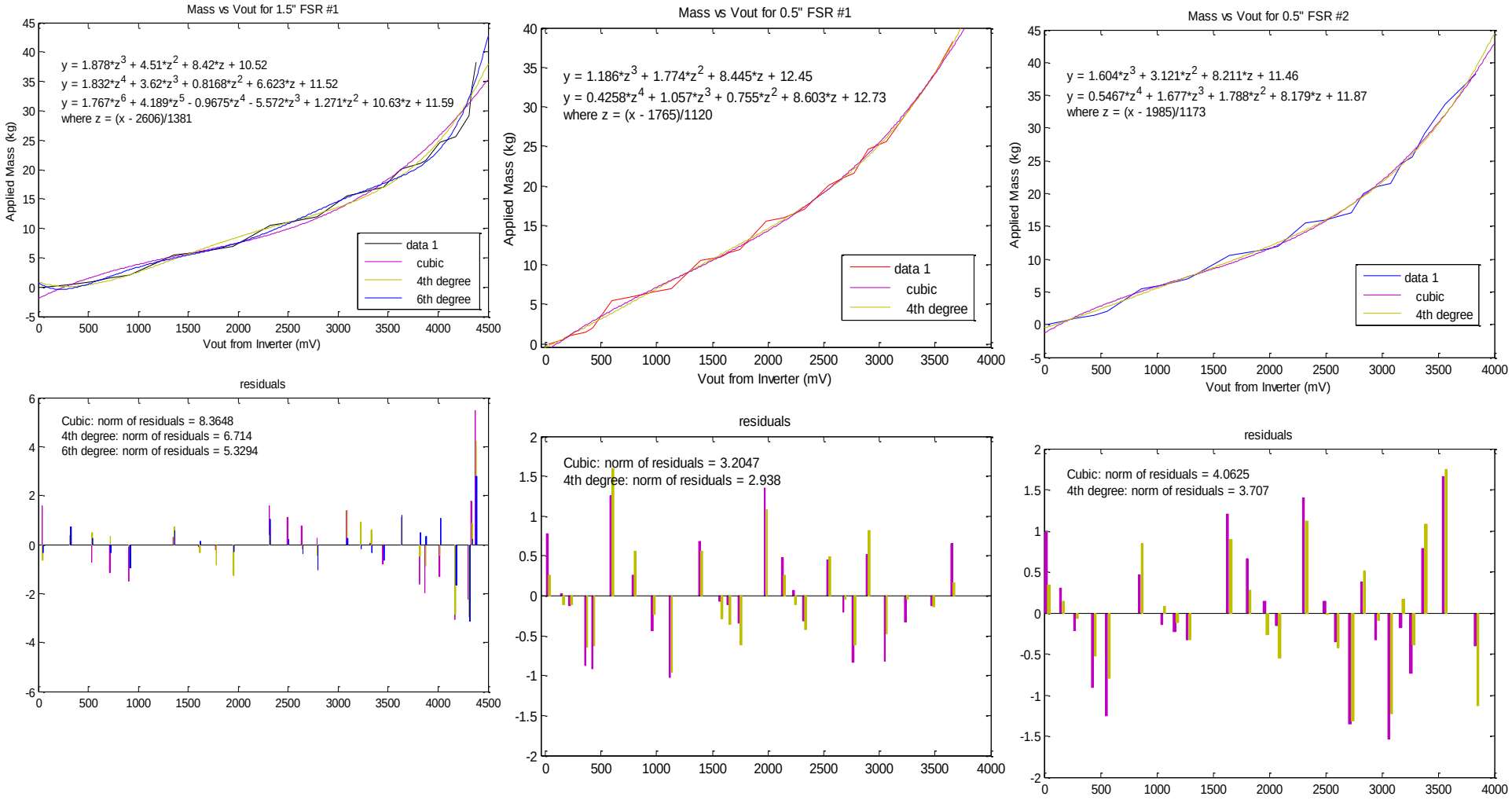

Figure 5.1 – Applied mass (kg) vs. voltage output (mV) for FSRs and their respective circuitry. Fitted curves also shown, as well as their corresponding residues. In each case the 4th degree polynomial curve was used, resulting in R^2 (fit) values of 0.9896, 0.9968 and 0.9950, respectively. The tables containing the values used to produce these graphs and equations can be found in Appendix A.2.

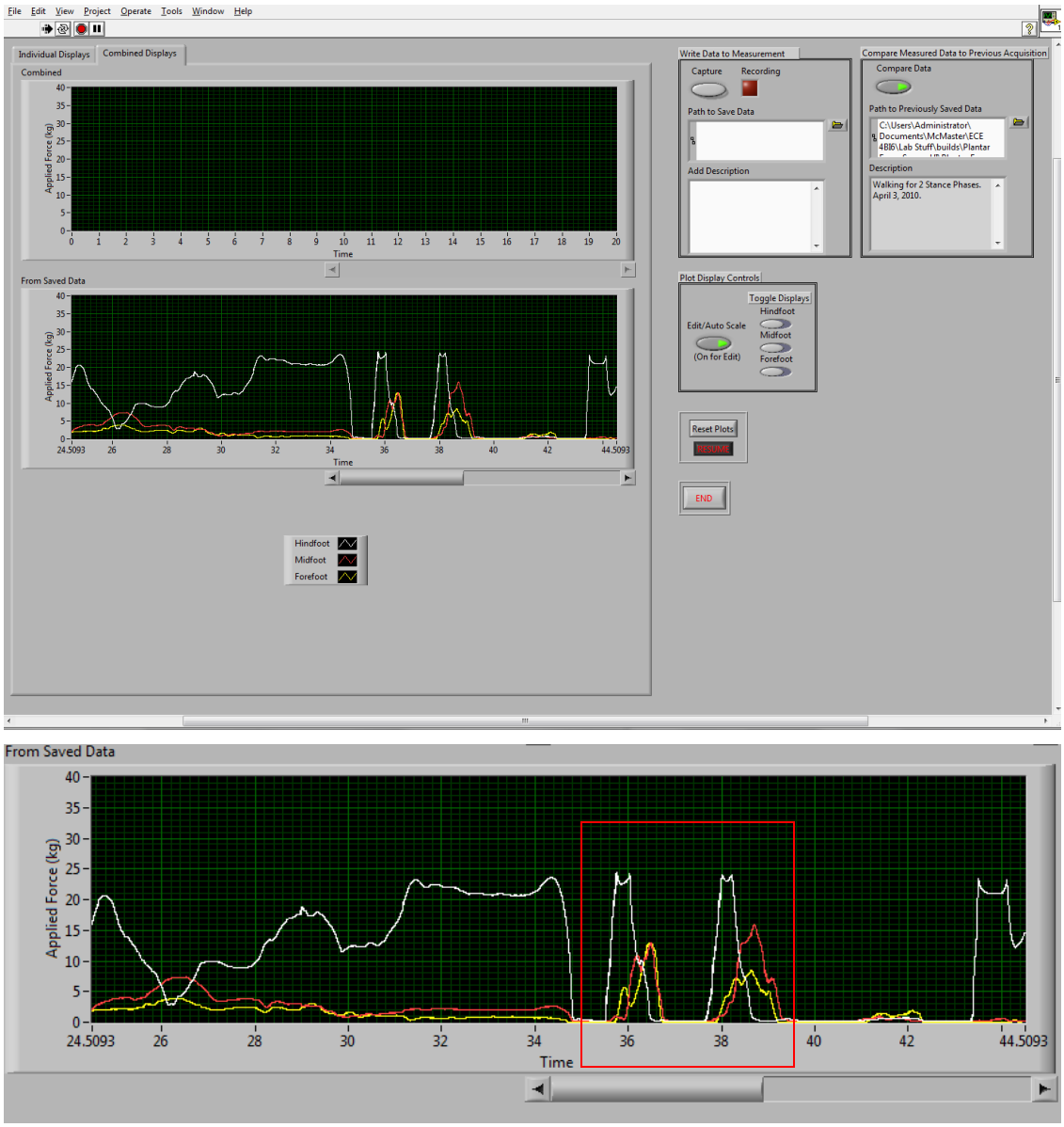

Figure 5.2 – Front panel of LabVIEW VI showing recorded measurement of 2 gait cycles (note that the midfoot and forefoot colours, red and yellow respectively, are reversed during this test due to an error when hooking up the device but are otherwise correct) and an enhanced view of the graph. The stance phases are indicated by the red box.

5.2 Discussion

5.2.1 Plantar Force Measurements

The documentation for the Interlink Electronics FSRs warns against excessive shear forces due to delaminating of the sensor layers but also because of the effect it can have on the sensor. Shear forces could cause misalignment of the layers of the FSR that are described in section 2.2 which would certainly have an effect on the overall resistance seen by the electrodes connected by the polymer semiconductors. Shear forces are particularly high at the hindfoot due to it being the initial contact site, so the foot still has forward momentum as it lands on the sensor [6]. The foot is relatively stable as it uses the hindfoot as a pivot during the landing, so the effect on the circular sensors at the mid and forefoot are less significant. This may explain why the square sensor at the heel is falling well short of its experimental values during operation. It is worthwhile to note that the proposed maximum current is exceeded on the heel sensor, though in the experimental phase this did not skew results, it is unknown how the additional current will interact with shear forces. If necessary, the current through the sensor could be reduced by adding some more circuitry before the inverting amplifier.

The effect of shear forces on the sensors could be quantified with specialized equipment to apply a known force at a known angle upon the surface of the sensor while the opposite surface is secured in place as it is in the PFS device. This would increase the complexity of calculations and require more sensors to determine the angle of incident forces on the foot but could feasibly correct the issue occurring at the heel. Input from the ankle range of motion sensor that the PFS is designed with could provide the angle of the applied force for instance, or the addition of an accelerometer could indicate the motion of the ankle prior to initial contact with the ground, and these values could be used by the system to calculate vertical forces using a more robustly calibrated sensor. However, the risk of delaminating and thus ruining the sensor still exists with large forces, such as those that could be produced during shear force calibration.

It is practical to note that the measurements were produced from the PFS while it was inside of a shoe worn by the subject, and that the calibration measurements were made with the sole sitting on a rigid surface instead of the sole of a shoe, which is more

elastic. This could be partially responsible for the altered effectiveness of the heel sensor, but is not reflected in the mid and forefoot sensors. Figure 2.1 shows that the average forces experienced by the heads of the metatarsal bones are equal to around 10% body weight and the first stance phase shown in Figure 5.2 shows these forces peak around 10 to 12 kg with a 75 kg subject which equates to 13 to 16%. This is only one iteration however, and as such further testing was required to qualify the accuracy of the mid and forefoot sensors and they do seem to be reasonably close to the expected values. Due to the length of the wires connecting the device it is difficult to acquire more than two stance phases, and in the aforementioned measurements the second stance phase is polluted by the subject stopping on their toes to turn around rather than displaying an error in measurement. Since these two sensors are working correctly, it seems unlikely that the elasticity of the sole of a shoe is to blame for the erroneous behaviour of the heel sensor.

Shear forces alone do not explain the shortcomings of the sensors and the range of applied forces that can be measured from them. It appears that the sensors are simply not suited for measuring weights greater than 40 kg distributed over their area, as the change in resistance is negligible or the resistance has saturated for forces larger than that. Using an alternate power supply to produce a 0.25 V drive voltage for the circuits did not yield any significant change in the sensitivity range of the sensors which seems to indicate that these values in Table 4.1 are the actual saturation resistances and correspond to maximum force readings. This is not completely surprising as the sensors do only show a resistance versus force relationship for applied weights up to 10 kg in their documentation, though it is stated that higher values are achievable no limit is given.

5.2.2 The PFS

The stance profiles in Figure 5.2 are likely measured from a non-standard gait, as the limitation of having wires connected from the PFS to a stationary device has an effect on the natural movements of a subject. The wires measure 1.5m in length and it is difficult to perform more than one stance phase within such a radius from the device circuitry and ADC. To get more realistic measurements from the device the wires need to be less stiff

and longer, or removed all together. The goal of this project was to demonstrate a proof of concept, and the wired nature of the device was implemented only for the proof design. Having the device be wired violates the specification that the device does not impede the natural motions of a subject.

Other than this physical limitation, the device and its programmed counterpart seem well suited for use in physiotherapy. The physical size and weight of the device are not an issue, weighing less than 200g and being 15.5 cm x 7.5 cm x 2 cm in dimensions it could easily be attached to a user's thigh by means of a strap without any significant impact on motion. There is no significant signal propagation delay among any of the sensors in the PFS or the ankle range of motion sensor which is important since the timing of the plantar forces was shown to be relevant in Chapter 2.

The LabVIEW component works exactly as desired and is extremely easy to use, requiring fewer than 5 user inputs to acquire, record and save measurements.

CHAPTER 6

CONCLUSIONS AND RECOMMENDATIONS

The design of a plantar force sensor for an ankle rehabilitation device using force sensing resistors is able to successfully acquire in-shoe measurements in the hind, mid, and forefoot sections and provide easily interpretable results. The device is able to be easily inserted into a patient's footwear without affecting plantar force distribution due to the uniformity and subtlety of the insert and sensors. However, the sensors used in this initial design are not well suited for measuring commonly occurring physiological forces of such a large magnitude as encountered on the sole of the foot. Furthermore, shear forces experienced during normal gait further diminish the effectiveness of the sensor placed under the heel. Beyond the shortcomings in the properties of the sensors, the device is effective at producing plantar force measurements within expected ranges in the mid and forefoot sections.

The design satisfies eight of the nine specifications, failing only to accurately measure large loads up to 100 kg. This includes repeatable and precise results and a total cost of under $40 CAD in this iteration. The software component of the device requires no prior experience to operate and is able to facilitate the archiving and comparisons required to properly track the rehabilitation of an injury to the ankle. With slight improvements in the device design and the technology of the sensors the objectives of the device could easily be completed.

The future iterations of the design have well defined goals. The sensors will need to be replaced with a model that can measure larger forces, such as the Tekscan Flexiforce A201. The device will need to be free of the physical limitations of being wired into the NI ADC, and as such will require a microchip with onboard ADC and a wireless controller to communicate with the software component. Finally, the number of sensors present on the device could easily be increased to provide more complete plantar force measurements to allow for more comprehensive analysis. Ultimately this iteration of the device acts as a successful proof of concept of an in-shoe plantar force sensor.

APPENDIX

A.1 Gait Cycle

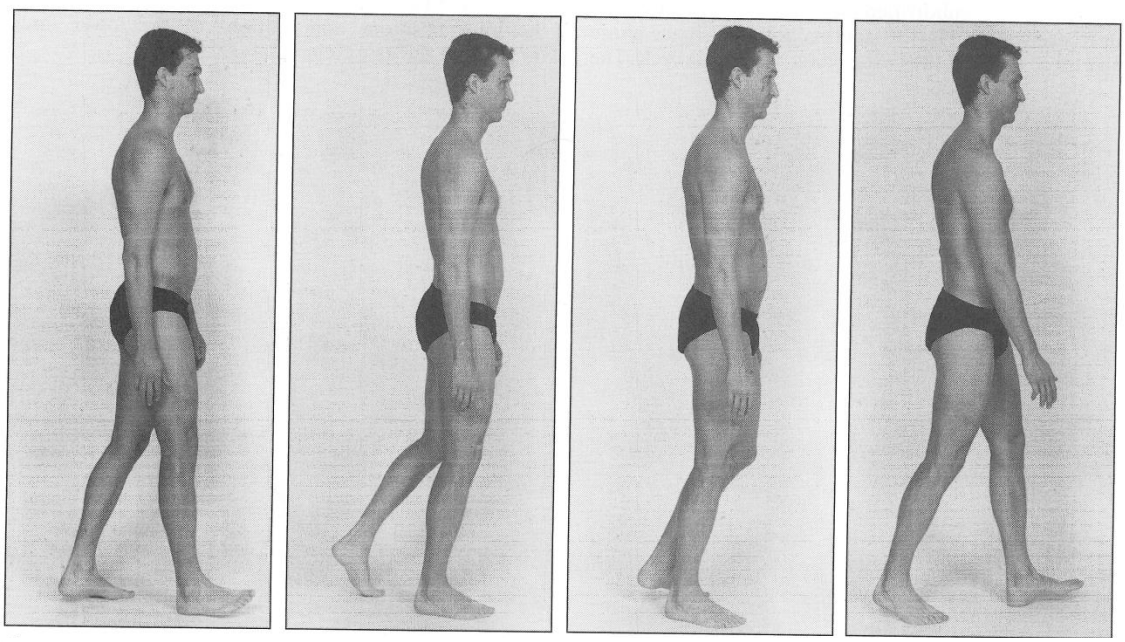

(1) (2) (3) (4)

Figures 1 to 4 represent the stance phase of walking. Figure 1 displays initial contact with the heel, figure 2 displays the loading response with the foot flat on the ground, figure 3 displays midstance with the opposite leg off of the ground and next to the foot, and figure 4 displays terminal stance with the foot preparing to enter the next phase. Figures 5 to 8 below represent the swing phase of walking. Figure 5 displays the preswing or toe-off with the foot pushing off of the ground, figure 6 displays initial swing, figure 7 displays midswing which corresponds to the other leg in midstance, and figure 8 displays terminal swing with the foot about to enter the initial contact phase. [5]

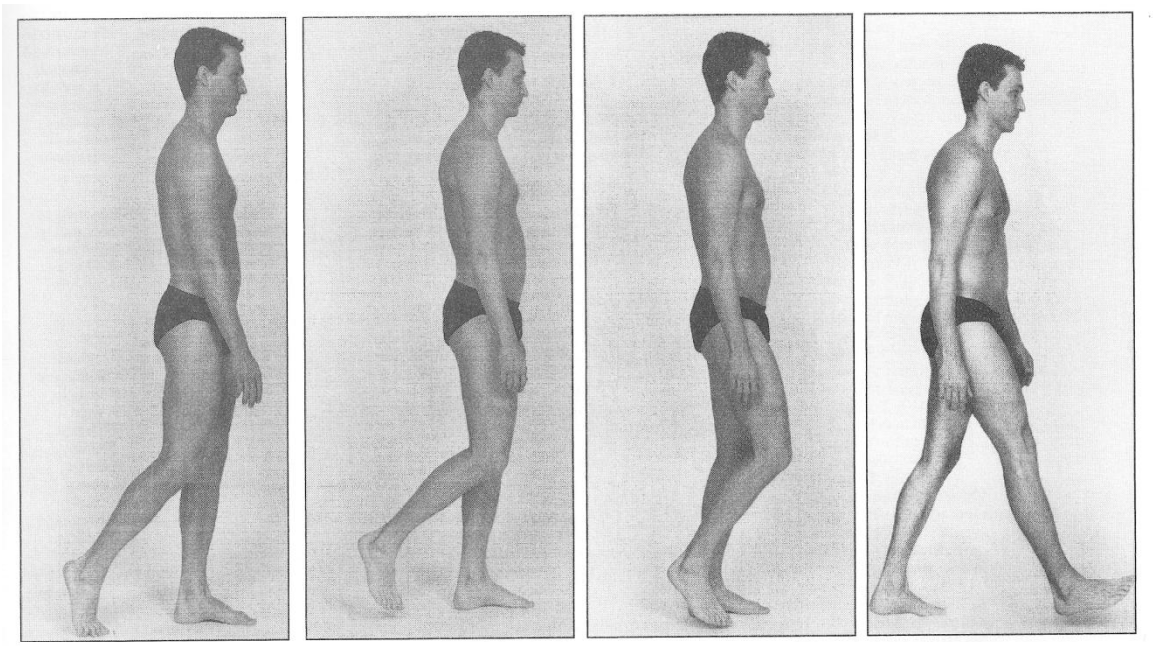

(5) (6) (7) (8)

Figure A.1 – The gait cycle.

A.2 Tabular Data for Applied Force versus Voltage Output for FSR

This table is the result of the averaging of the repeated tests done to each sensor to determine the output voltage with respect to the applied mass. Each sensor was activated at least five times with each of the masses listed here as described in Chapter 4, and the average value was taken to determine the voltage versus force curve for the circuit.

Table A.1 – Tabulated data from calibration experiment.

	Average Output Voltage (mV)			
Applied Mass (kg)	0.5" #1	0.5" #2	0.5" #3	1.5"
0	30	30	30	44
0.5	156	160	160	320
1	225	283	250	540
1.5	367	442	400	720
2	431	566	490	912.6667
5.5	599	860	740	1359.333
6	800	1060	940	1616.667
6.5	970	1170	1060	1783.333
7	1130	1283	1188	1953.333
10.5	1395	1644	1425	2316.667
11	1575	1815	1635	2500
11.5	1650	1970	1750	2640
12	1750	2080	1894	2793.333
15.5	1980	2319	2255	3090.667
16	2140	2505	2365	3226.667
16.5	2239	2599	2510	3331.333
17	2330	2730	2600	3453.333
20.045	2545	2835	2880	3633.333
21.045	2685	2960	3080	3819.333
21.545	2775	3075	3185	3874.667
24.59085	2900	3180	3390	4020
25.59085	3059	3270	3500	4174.667
29.13625	3246	3380	3661	4313.333
33.68165	3480	3560	3880	4379.333
38.22705	3660	3840	4070	4379.333

A.3 LabVIEW VI

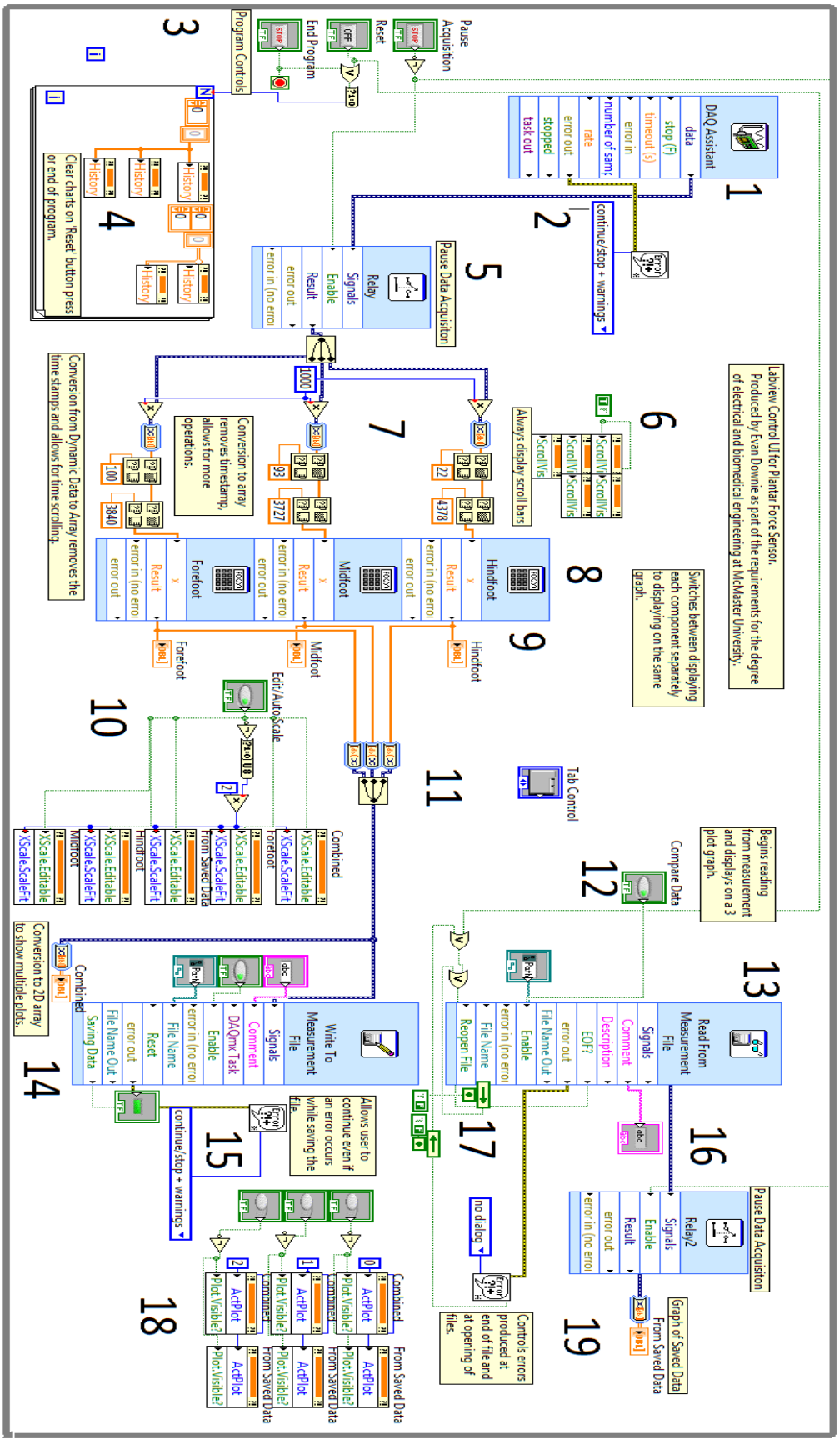

Figure A.2 – Plantar force sensor LabVIEW VI block diagram.

Figure A.2 displays the block diagram (which comprises the code) of the plantar force sensor's standalone LabVIEW virtual instrument. Since the comments within the code are too small to display in the report the blocks in the diagram have been numbered and will be explained here.

1 – The DAQ Assistant – This VI block reads data from the NI ADC. For this project channels ai0, 2 and 4 were used with voltage ranges of 0 to 5 V. Samples are read continuously at 1 kHz with a 100 sample buffer. Due to continuous running the block cannot be disabled by a simple switch.

2 – General Error Handler (DAQ Assistant) – This block handles any errors generated by block 1. In this case the errors are set to display to the user, usually indicating the lack of an attached ADC, and the user can decide to continue or stop the program.

3 – Program Controls – This block contains three switches that are represented on the front panel. The topmost switch controls the relay blocks indicated by 5 and 16 by either enabling or disabling them. The middle switch operates as a latch and controls blocks 4 and 13. Block 4 is a for loop and thus requires an unsigned integer and not a Boolean value, as such the output from the middle switch is converted to indicate a 0 or 1 to control the iterations of this loop. Block 13 is the 'read' block and the middle switch controls file reopening. The bottom switch is also a latch and controls the entire program, and pressing it will end execution, however before doing so it also causes block 4 to run once.

4 – Plot Memory – Block 4 is a for loop structure controlled by block 3. Inside the for loop are 5 property nodes which are linked to each plot in the program. A blank array is attached to the input of each property node, which will clear the memory contents of the plot while the loop is running. The control from block 3 operates as a latch and thus a value of 1 will be passed to the loop for one program cycle, causing it to clear the plot memories and stop.

5 – DAQ Relay Block – This express VI controls the dynamic data type that is wired into it by either allowing or stalling its propagation. This means when the block is enabled the signal runs through unimpeded, but when the block is disabled it is paused. In this

program the relay block sets the output to a dynamic data type with value 0 when it is disabled.

6 – Scroll Bar Block – This block simply turns the scroll bars for each of the plots on indefinitely so that a user cannot accidentally disable them. A constant Boolean of 'true' is wired into 5 property nodes.

7 – Data Manipulation Block – This block first splits the dynamic data type from block 1 into the first 3 signals contained within (the only ones in this case) and multiplies them by 1000 to convert their values into mV. Next, the signals are converted to a 1-D array of integers; this removes the time data from the dynamic data type and allows for easier manipulation of the signals such as in the next step. Finally, the signals are confined to the respective voltage range determined during the sensor testing, as the equations relating force to voltage are only valid inside that range.

8 – Curve Fitting – Here each of the 1-D arrays is fed into a formula express VI which uses the input in the respective curve fitting equations determined during sensor calibration. These blocks could have been implemented with simple algebraic blocks but this would have been a needless complication. 3 separate blocks need to be used since only one stream can be output.

9 – Waveform Charts I – From top to bottom next to the curve fitting blocks are waveform graphs displaying the hindfoot, midfoot and forefoot. These graphs are configured to scale the time axis by $1/1000^{th}$, which corresponds to the sampling rate and produces graphs in the front panel that show the signal against real time.

10 – Auto-scale Control – This block includes a switch and 10 property nodes, 2 for each waveform graph in the block diagram. The switch controls the Boolean input to the 5 property nodes that control the editing of the x-axis of the corresponding chart. The 'not' of the switch is converted to an unsigned 8-bit value and wired into the 5 remaining property nodes that control the continuous auto-scaling of the x-axis of the corresponding graph. The result is that when the switch is on the x-scales can be changed by the user to the desired ranges, and when it is off the graphs follow the signal over the range specified by the user's editing.

11 – Recombination – This block converts the 1-D arrays back into dynamic data types by adding the time-stamp, and then combines them into a single signal to be fed along the program. This combined signal is fed into block 14 as well as the waveform chart next to it, which will display all signals simultaneously after conversion to a 2-D array. The blue block above this label is the 'Tabs' block which can control the visible tabs on the front panel but in this program is controlled manually.

12 – Data Comparison Switch – This switch feeds into block 13 and controls the displaying of measurements read from previous files on the corresponding waveform chart.

13 – Read from File Block – This block is an express VI that reads from a measurement file either produced by this program or some other graphing program. A file path block is linked to this VI that allows a user to search for the file to be read on any hard drives or networks connected to the computer. Additionally the description of the file is displayed on the front panel so a user can easily archive their records. A header in the file contains all relevant information needed to read the signals within including time-stamps and sampling rate. This block also outputs a Boolean value to indicate when the end of a file has been reached, which is fed back into the block to reopen the file when this occurs.

14 – Write to File Block – The combined signal from block 11 is fed into an express VI that writes dynamic data types to a file specified by the user. This block will write the header for the file as well as any comments in the comment field from the front panel (shown in pink on the block diagram) to a file of name, type and location specified by the user in the file path block that is connected to this block.

15 – General Error Handler (Writing) – this block handles errors for block 14 in the same way that block 2 does for block 1. This block will prevent errors such as non-existent directories from ending the program and will rather allow the user to correct the error.

16 – Read Relay Block – This block controls the signal being read from block 13 in much the same way that block 5 does for block 1.

17 – General Error Handler (Reading) - This block handles errors for block 13, but does not display messages to the user. The errors produced by block 13 consist of reading from a file past the end of file marker, when no file path is selected the block simply displays a signal of 0. This block has a feedback input into block 13 which will reopen the specified file if an error occurs.

18 – Plot Display Controls – This block contains 3 switches wired into 3 property nodes corresponding to the 2 waveform charts that display all 3 signals at once, one from the ADC and one from the file being read. Each property node has a constant value wired into the node to select which plot for the corresponding chart it is affecting, and the switch controls the visibility of that plot.

19 – Graph of Read Data – This block converts the data read from the measurement file to a 2-D array and displays it on a waveform graph showing all 3 plots at once.

The block diagram of the LabVIEW VI designed to incorporate both devices was derived from the PFS standalone VI so only significant additions will be noted as the rest of the block can be assumed to operate as previously explained. The notes here correspond to the notes in Figure A.4. The block diagram and front panel of the ankle rehabilitation monitor VI can be found at the end of this appendix in Figures A.3 and A.4.

1 – Auto-Scale Control – Moved block 10 to a different location.

2 – Range of Motion Curve Fitting – Added 2 more equation blocks to handle the range of motion voltage readings.

3 – Waveform Charts – Removed the individual displays, now only display range of motion, plantar forces, or both across 3 separate tabs.

4 – Case Structure – This case structure switches between showing real time acquisitions or reading from a second measurement file in order to compare two saved measurements.

5 – Second Read From Measurement File – Added another block similar to block 13 in the PFS VI, which allows the user to compare two previously saved files.

6 – Second Measurement Relay Block – Allows the user to pause acquisition from the second saved file to facilitate comparison.

7 – Plot Display Controls – Added 2 more sets of plot displays to toggle plantarflexion and inversion displays.

8 – Signal Splitting After Read – In this VI the signals are split into range of motion, plantar forces and combined plots to be displayed against real time values when read from the first measurement file.

Below is the front panel display for the combined ankle rehabilitation monitor VI. Note the extra block to enable the display of two measurement files simultaneously. The block diagram for this VI can be found on the next page.

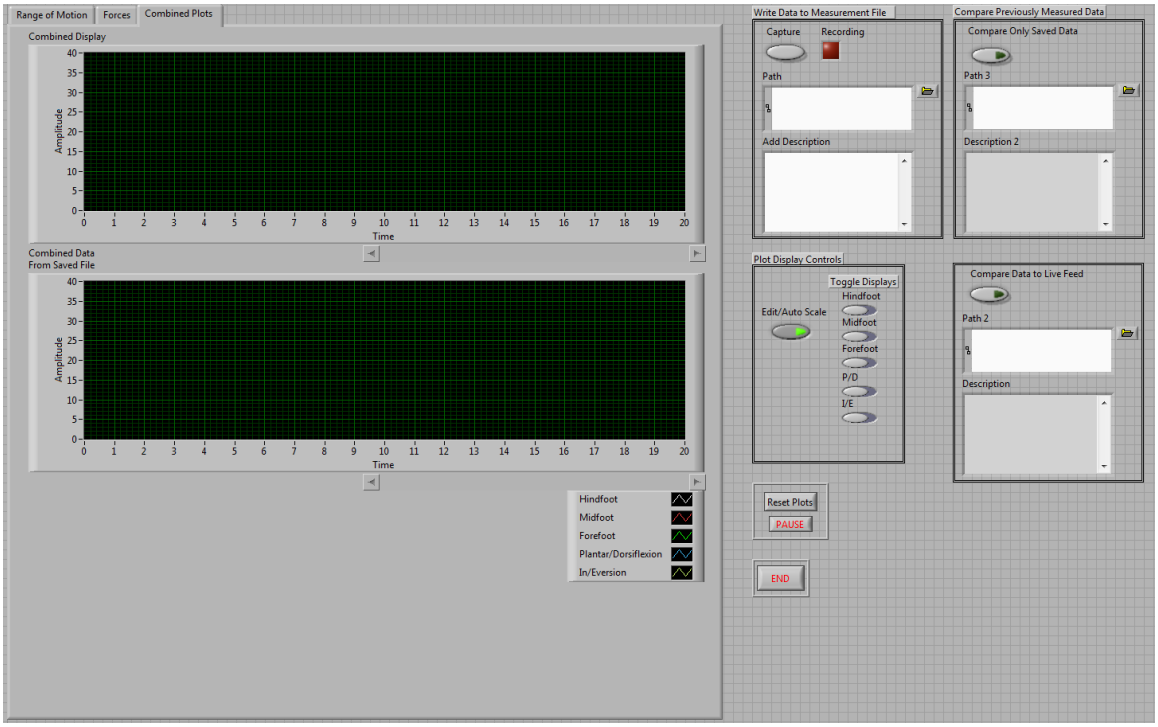

Figure A.3 – Ankle rehabilitation monitor LabVIEW VI front panel.

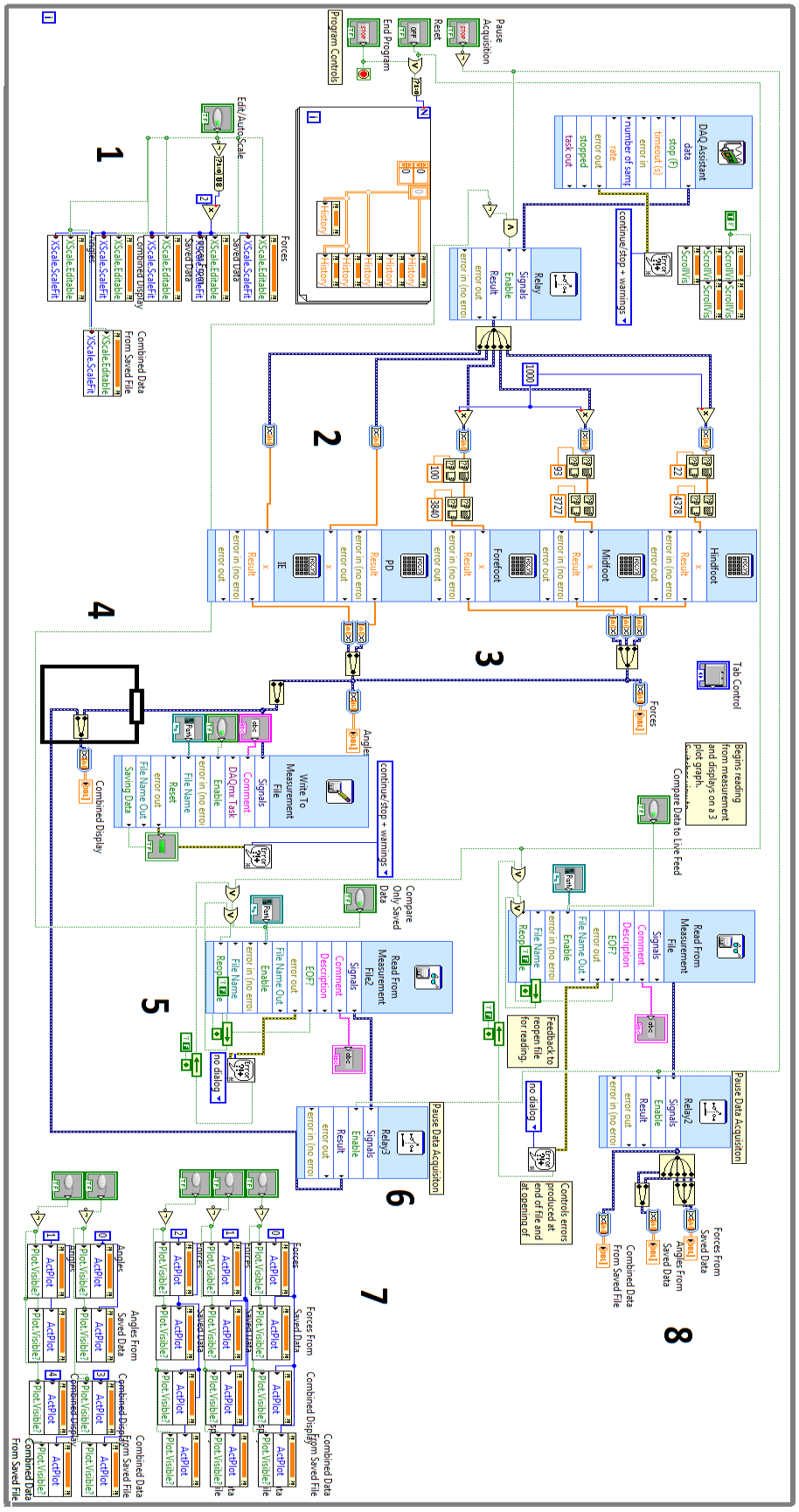

Figure A.4 – Ankle rehabilitation monitor LabVIEW VI block diagram.

REFERENCES

(1) K L, Pamela, Norkin CC. Joint structure and function: a comprehensive analysis. 3rd. ed. Philadelphia: F.A. Davis; 2001.

(2) Hurkmans HLP. Techniques for measuring weight bearing during standing and walking. Clin.Biomech. 2003;18(7):576.

(3) Yavuz M. Plantar shear stress distributions: comparing actual and predicted frictional forces at the foot-ground interface. J.Biomech. 2007;40(13):3045.

(4) Thornquist, Eline. Diagnostics in physiotherapy – processess patterns and perspectives, part II. Advances in Physiotherapy. 2001 Dec:3(4):151-162

(5) Clarkson HM. Musculoskeletal assessment: joint range of motion and manual muscle strength. 2nd ed. Philadelphia: Williams & Wilkins; 2000.

(6) Ledoux WR, Hillstrom HJ. The distributed plantar vertical force of neutrally aligned and pes planus feet. Gait and Posture 2002;15(1):1-9.

(7) Nyska M, Shabat S, Simkin A, Neeb M, Matan Y, Mann G. Dynamic force distribution during level walking under the feet of patients with chronic ankle instability. Br.J.Sports Med. 2003;37(6):495-497.

(8) Interlink Electronics force sensing resistor (FSR). [Online]. 2006-2010 [Cited 2010 Apr 20]; Available from: URL: http://www.interlinkelectronics.com/force_sensors/technologies/fsr.html

(9) Hall RS, Desmoulin GT, Milner TE. Technique for conditioning and calibrating force-sensing resistors for repeatable and reliable measurement of compressive force. J Biomech 2008 Sept:41:3492-3495.

(10) Flexiforce: Single Button Force Sensing Resistor. [Online]. 2007 [Cited 2010 Apr 20]; Available from: URL: http://www.tekscan.com/flexiforce/flexiforce.html

(11) Hollinger A, Wanderly MM. Evaluation of commercial force-sensing resistors. IDMIL McGill U 2006 Jan: Unpublished.

(12) Jasper S de Vries, Rover Krips, Inger N Sierevelt, Leendert Blankevoort, C N van Dijk. Interventions for Treating Chronic Ankle Instability. John Wiley & Sons, Ltd., Amsterdamn, Noord-Holland, 2009.

(13) Nieuwboer A, De Weerdt W, Dom R, Peeraer L, Lesaffre E, Hilde F, et al. Plantar force distribution in Parkinsonian gait: a comparison between patients and age-matched control subjects. Scand.J.Rehabil.Med. 1999;31(3):185.

(14) Sawacha Z, Gabriella G, Cristoferi G, Guiotto A, Avogaro A, Cobelli C. Diabetic gait and posture abnormalities: A biomechanical investigation through three dimensional gait analysis. Clin.Biomech. 2009 200911;24(9):722-728.

(15) University of Virginia health system: Foot pain and problems. [Online]. 2010 [Cited 2010 Apr 12]; Available from: URL: http://www.healthsystem.virginia.edu/uvahealth/adult_orthopaedics/footpain.cfm

(16) GE Healthcare: Medcyclopaedia: Foot. [Online]. 2010 [cited 2010 Jan 31]; Available from: URL: http://www.medcyclopaedia.com/library/topics/volume_iii_1/f/foot.aspx

VITA

NAME:	Evan Downie
PLACE OF BIRTH:	Toronto, Ontario
YEAR OF BIRTH:	1986
SECONDARY EDUCATION:	Barrie North Collegiate, (2000-2004)
HONOURS and AWARDS:	Honor Roll, 2000-2003
	Ontario Scholar, 2004
	Pepsi© Physics Award, 2004
	Dean's Honours List, 2007-2009